Influence of the Boundary Resistance and Pair Breaking on Josephson Coupling in HTS Weak Links

MIKHAIL KUPRIYANOV

Institute of Nuclear Physics, Moscow State University, Moscow, 119889, GSP, Russia

ABSTRACT

The experimental investigation of the properties of the HTS junctions have confirmed the existence of the new effects which have never observed in the LTS junctions (the influence of the boundaries on the properties of the structures; suppressed I_cR_n products; scaling low; the long-range proximity effect; nonmonotonic behavior of the critical current upon thickness of the ferromagnetic interlayer materials). The goal of this work is to analize possible reasons of this effects. We start with the discussion of the boundaries problems and then turn to the processes in the weak link materials.

KEY WORDS: HTS Josephson junctions, proximity effect, pair breaking.

I. THE BOUNDARIES.

The problems of the boundary fabrication stand in the central of the development of the HTS Josephson junction technology. Their importance for all types of the HTS junctions directly follow from the intrinsic properties of the HTS materials (small coherence length; high chemical activity; anisotropy; high values of the resistivity compare to the one in ordinary normal metals. It is obvious that in order to have the HTS junctions with reprodisible parameters one must exclude any chemical reaction in the vicinity of the boundaries. But even in this case the mismatch between the crystal lattices of the HTS superconductors and the interlayer material can result in the formation rather thick nonsuperconducting layers in the near boundary region.

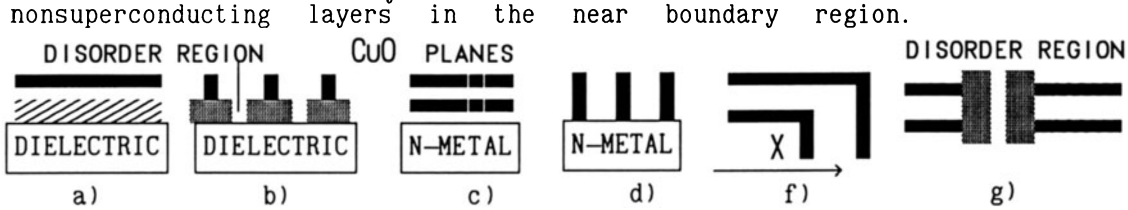

Fig.1. Various typical schemes of the HTS Josephson junction's boundaries.

The special investigations have shown [1-6] that during the growth of the C-oriented YBCO films on the dielectrics $SrTiO_3$ or YSZ the mismatch between the crystal lattices results in the large mechanical tensions at the interface leading to the formation of the stable oxygen deficit N-layer (disorder region on Fig. 1a). Since the coherence length of the HTS materials $\xi_\perp$ is smaller or comparable with the thickness of this layer it is clear that the problem of the conservation of the superconductivity on the atomic scale in the vicinity of the boundary during the junction's fabrication is very serious. The simple changing of the C axis orientation (see Fig. 1b) does not lead to the solution. The losses of the periodicity of the CuO planes in C-direction due to the irregular mechanical tension in the vicinity of the boundary result in the formation of the rather thick (1.5 ÷ 2 nm) layer in which the crossover from three to two-dimensional types of conductivity takes place. This leads to the enhancement of quasiparticle reflection from this region and as a result to the formation of the large effective thickness of the I-layer in the SIS junctions.

In the single grain boundary junctions in C-oriented HTS thin films or fabricated on bicrystal subsrates the same crossover should takesplace (see Fig. 1g) resulting in formation the weak link regions with relatively large $R_n \approx$

Y. Bando et al. (eds.), *Advances in Superconductivity V*

$10^{-7} \div 10^{-8} \Omega cm^2$. The larger the asymmetry of the crystal lattices relative to the boundary the larger their mismatch at the boundary and as a consequence, the thicker the disordered layer. The same localization of the carriers in CuO planes is responsible for the resistance of the "clean" 90° grain boundary (see Fig.1f) [7,8] leading to expression

$$R_N^{-1} \approx \frac{e^2\alpha}{2\pi\tilde{d}} (\alpha^2-1)^{3/2}, \quad \alpha = (2\tilde{d}/\lambda^*). \tag{1}$$

which fits well the experimental data ($R_n \approx 10^{-7} \div 10^{-8}$ Ωcm^2) under condition $\alpha \approx 1 + (1 \div 5)\ 10^{-3}$ or $\lambda^* \approx 2\tilde{d} \approx 5$ A (λ^* is de-Brogile wavelength of the quasiparticles , $\tilde{d}$ is the effective thickness of the CuO plane). Such a crossover is the intrinsic property of the high anisotropic HTS materials and has to be in any situation then the periodicity in C-direction is breakdown due to any reasons e.g. due to mismatch of the crystal lattices at the boundaries.

For the atomically sharp and "clean" (without disorder regions) boundaries (Fig 1c, 1d) we can also have large R_n thanks to the difference of the Fermi-velocities of the materials at HTS/(Ag,Au) interfaces. Assuming that the HTS/(Ag,Au) boundary's transmission coefficient $D(\theta)$ is small for the estimation of the specific boundary resistance R_B we can use the expression [8]

$$R_B^{-1} = \frac{e^2 p_N^2}{2\pi^2\hbar^3} \int_0^{\theta_0} D(\theta,\alpha) \sin\theta\cos\theta \, d\theta, \quad \theta_0 = \arcsin\left[\frac{(p_\perp^2\cos^2\alpha + p_\parallel^2\sin^2\alpha)^{1/2}}{p_N}\right], \tag{2}$$

where θ and α are the angles between the normal to the boundary and the direction of the Fermi-momentum of the quasiparticles in N-metal p_N and C-axis respectively, $p_\perp$ and $p_\parallel$ are the components of the Fermi-momentum in HTS material in C-direction and in CuO planes.

In situation shown on Fig.1c the solution of the Schrodinger equation leads to the wellknown expression for $D_\perp(0,0)=4v_\perp v_n/(v_\perp+v_n)^2$, where $v_\perp = p_\perp/m_\perp$, $v_n = p_N/m_e$. Since in HTS materials $p_\perp \ll p_N$, and $\theta_0 \approx p_\perp/p_N \ll 1$ from (2) for the typical values of the parameters $v_n \approx 10^6$ m/c, $m_\perp \approx 100\ m_e$, $p_\perp \approx 5\text{x}10^4$ m/c it follows:

$$R_{B\perp}^{-1} \approx \frac{e^2 p_N^2}{4\pi^2\hbar^3} D_\perp(0,0)\ \theta_0^2 \approx \frac{e^2 p_\perp^2}{\pi^2\hbar^3} \frac{v_\perp}{v_n} \approx 10^7\ \Omega^{-1}cm^{-2}. \tag{3}$$

The boundary shown on Fig.1d can be considered as the interface between the isotropic N-metal and the diffraction lattice formed by the CuO planes. In this case the transmission coefficient can be roughly estimated by using the diffraction lattice formula

$$D_\parallel(0,\pi/2) = 4\ (v_\parallel/v_n) \frac{\sin^2((\pi d^*/\lambda)\sin\theta)}{((\pi d^*/\lambda)\sin\theta)^2} \frac{\sin^2((M\pi d^*/\lambda)\sin\theta)}{\sin^2((\pi d^*/\lambda)\sin\theta)}, \tag{4}$$

where $v_\parallel = p_\parallel/m_\parallel \ll v_n$ ($p_\parallel \approx 5\text{x}10^5$m/c; $m_\parallel \approx 10\ m_e$) is the Fermi-velocity of the quasiparticles in CuO planes, d^* and λ are the lattice constant and de-Brogile wavelength in the N-metal respectively, M is the number of the planes. Since the main contribution to the integral (2) falls on the $\theta \le \lambda/Md^*$ we have

$$R_{B\parallel}^{-1} \approx \frac{e^2 p_\parallel^2}{4\pi^2\hbar^3} D_\parallel(0,\pi/2) \left[\frac{\lambda^*}{d^*\ M}\right]^2 \approx 10^{10}\ \Omega^{-1}cm^{-2}. \tag{5}$$

Here $\lambda^* \approx d^* \approx 5$ A is the de-Brogile wavelength of the quasiparticles in CuO planes.

The large values of the specific boundary resistance are responsible for the suppression of the I_cR_n product in HTS Josephson junctions.

2. HTS WEAK LINKS WITH THE NOBLE METALS.

The theoretical estimations (3),(5) as well as the experimental data have shown that the properties of the HTC weak links determined by the suppression parameter $\gamma_B = R_B/\rho_N\xi_N^*$ where ρ_N and ξ_N^* are the normal-state resistivity and coherence length of the N-metal [7-13]. This parameter is responsible for the proximity effect at YBCO/Au,Ag boundaries and relatively large depending on the C axis of HTS material is perpendicular ($\gamma_{B\perp} \approx 10^4$) or parallel $\gamma_{B\parallel} \approx 20$ to them.

For the SNS sandwiches the calculations in the limit of small thickness of the junction $L \ll \xi_N^*$ and large $\gamma_B \gg \max\{1,\gamma\}$ lead to [7,8]

$$\frac{eV_c}{2\pi T_c} = \frac{T}{T_c} \max_{\varphi} \sum_{\omega>0} \frac{\Delta^2 G_S \sin(\varphi)}{\omega[\omega^2(1+2\gamma_{BE}\omega/(G_S 2\pi T_c))^2+\Delta^2\cos^2(\varphi/2)]^{1/2}}, \quad G_S=\omega/(\omega^2+\Delta^2)^{1/2}, \tag{6}$$

$$R_N = 2\rho_N\xi_N^*(\gamma_{B1}+\gamma_{B2}), \quad \gamma_{BE}=\gamma_{ef}(L/\xi_N^*), \quad \gamma_{ef} = \gamma_{B1}\gamma_{B2}/(\gamma_{B1}+\gamma_{B2}),$$

where φ is the phase difference of the superconductor order parameters, $\omega = \pi T(2n+1)$ are the Matsubara frequencies, γ_{B1} and γ_{B2} - suppression parameters of the interfaces. From (6) it follows that

$$R_N \propto (\gamma_{B1}+\gamma_{B2}), \qquad I_c \propto (\gamma_{B1}\gamma_{B2})^{-1}, \tag{7}$$

leading for the symmetric structures ($\gamma_{B1}=\gamma_{B2}$) to the scaling low

$$V_c = I_c R_N \propto R_N^{-1} \propto I_c^{1/2}, \tag{8}$$

while in the case $\gamma_{B1} \gg \gamma_{B2}$ the characteristic voltage

$$R_N \propto \gamma_{B1}, \qquad V_c \propto \gamma_{B2}^{-1}, \tag{9}$$

depends only on the properties of the boundary with better transparency. The last result shows that to obtain the junction with good parameters it is sufficient to have only one boundary with high transparency.

Figure 2 shows that the experimental data are fitted well by the theoretical curves calculated from (6) result in $\gamma_{BM} \approx 10$ and 150 [15,16]; ≈ 50 [17] $\gamma_{ef} \approx 75$ [19], ≈ 200 [18] and ≈ 10 [15]. It is interesting to note that the $I_c R_N$ product of the extremely asymmetric SNS junctions [15] is two times smaller the symmetric one [14] with $\gamma_{BM} \approx \gamma_{ef}$. This fact directly follows from (6) confirming once again the applicability of the theoretical model to the description of the properties of the HTS weak links based on noble metals (Au, Ag). Using the experimenta values $\rho_N\xi_N^*$ product, normal junction resistance R_N and estimated γ_{BM} it is possible to calculate the real cross-section $S_r = \rho_N\xi_N^*/R_N$. In all cases [15-19] S_r turns out to be at least ten times smaller then geometrical one suggesting that the boundaries of the structures are rather inhomogeneous.

3. HTS WEAK LINKS WITH THE N-OXIDE INTERLAYERS.

The processes in the HTS weak links with N-oxide interlayers [20,21] is more complicated due to the experimentally observed long range proximity effect that is temperature independent and larger than the estimated from the transport properties of the materials decay lengths ξ_{ef} ($\approx$65 nm for $La_{1.5}Ba_{1.5}Cu_3O_{7-y}$ [20, 21]; $\approx$ 10 nm for $Y_{0.6}Pr_{0.4}Ba_2Cu_3O_{7-\delta}$ [23]; $\approx$ 5÷8 nm $PrBa_2Cu_3O_{7-\delta}$ [19-26]). It is hardly surprising that the decay length can be so large since it goes to infinity then T goes to zero both in clean ($\xi \propto T^{-1}$) and dirty ($\xi \propto T^{-1/2}$) limits. The surprising fact is the observed it's temperature independence [20-26].

In the BCS based theories this fact could explain by taking into account the temperature independent pair breaking in N-region, e.g. paramagnetic impurities, which removal of divergence in $\xi_N(T)$ leading to ($T_{cN}=0$):

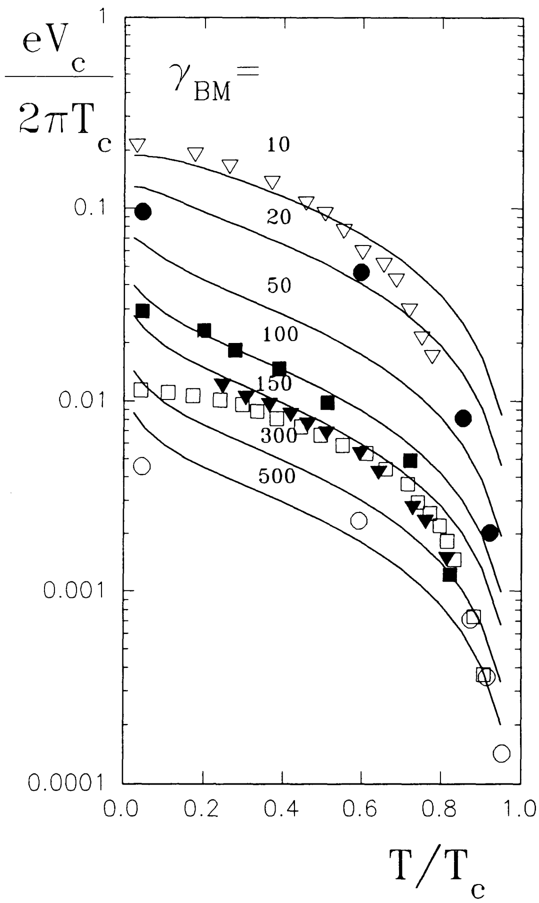

Fig.2. Temperature dependence of the critical current of the SNS junction for various values suppression parameter γ_{BM}. The symbols are the experimented data from [14] (∇,▼), [15] (O,●), [17] (□), [19] (■).

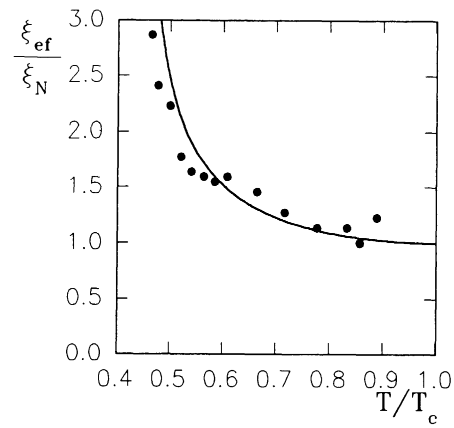

Fig.3. The temperature dependence of the effective decay length (18). The symbols are the experimental data [19].

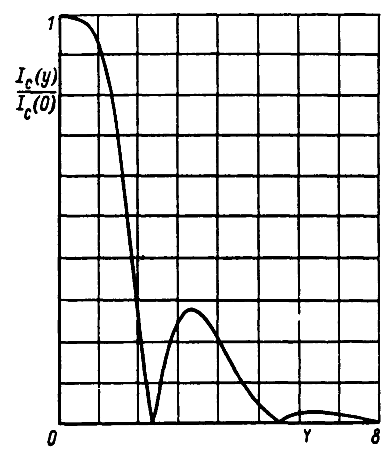

Fig.4. The dependence of the critical current SNS junction with ferromagnet interlayer upon the distance between electrodes [28].

$$\xi_{ef} = \xi_N^* (1/q + T/T_c)^{-1/2}, \qquad \xi_N^* = (D_N/2\pi T_c)^{1/2} \qquad q = \pi T_c \tau_s, \tag{10}$$

where τ_s is the spin flip time. Due to the large T_c a small concentration of paramagnetic impurities is sufficient to have in wide temperature interval practically constant $\xi_{ef} = \xi_N^* q^{1/2}$.

$$\xi_{ef} = \xi_N^* q^{1/2}. \tag{11}$$

Since the concentration x of the paramagnetic centers in PrBaCuO twice larger than the critical one in $Y_{1-x}Pr_xBa_2Cu_3O_{7-y}$ ($x_c \approx 0.5 \div 0.6$ or $q \approx 3.6$) it is reasonable to suppose that in PBCO the parameter $q_* \approx 2$ and from (11) for the decay length gets the value $\xi_{N\|}^* \approx 3 \div 5$ nm close to $\xi_\|$ in YBCO.

At small electrode spacing L the temperature dependence of the I_cR_N product (see Fig.2) fits well by the formula (10) with $\gamma_{ef} \approx 50$. At larger $L \geq \xi_{ef}$ better fitting can achieved with the predictions of the SNINS model [19] with the paramagnetic impurities in N-regions.

Summarize all this facts it is possible to conclude that the properties of the edge junctions with PBCO interlayer is close to that of the SNIS structures with the paramagnetic centers in N region where role of the I layer is played by the ex situ made boundary.

The critical temperature of $Y_{0.6}Pr_{0.4}Ba_2Cu_3O_{7-\delta}$ using as the interlayer in edge type junction [23] is close to $T_{cN} \approx 45$ K which corresponds to $q \approx 5$. In this case following from the BCS theory temperature dependence of the effective decay length is more complicated then (14) and in accuracy of 5% can be approximated by the expression

$$\xi_{ef}(T) = \xi_N^* \left[\frac{T_c - T_{cN}}{T - T_{cN}} \frac{\pi\tau_s T_c}{1 + (4/\pi^2)\pi\tau_s(T_c - T)} \right]^{\frac{1}{2}}. \qquad (12)$$

which fits well the experimental dependence [23] (dots on Fig.3) leading to coherence length close to the one in CuO planes of YBCO $\xi_N^* \approx \xi_{ef}(T_c)q^{-1/2} \approx 45$ Å

The variety of nonsuperconducting oxides opens new possibilities in investigations of the new effects in Josephson structures with ferromagnetic weak link materials [27]. The junctions have shown the nonmonotonic behavior of the critical current upon their thickness d. It increases from ≈5 mA at d ≈ 20 nm up to ≈ 100 mA at d ≈ 50 nm and then fall off at higher d.

The theory [28] predicts that this fact could be quantitatively explain by the complex value of the decay length in ferromagnets leading to the Ic(d) dependence shown on Fig.4. In odd periods of the Ic(d) the properties of the junctions are close to the ordinary one while in the even periods we should have the so-called "π"-contacts.

4. SINGLE GRAIN BOUNDARY JUNCTIONS.

The scope of the experimental data [8,9] obtained in single grain boundary junction can be understood by taking into account the the wave nature of the charge carriers. As it follows from the first paragraph it is the diffraction effects that responsible for high values of the normal junction resistance. The suggestions that it determines by the relatively large (in comparison with the lattice constant) thickness of the I-layer like in SIS junctions or by the difference of the Fermi-velocities like in SNS structures is inconsistent with the TEM analysis of the boundary structure which definitely confirm the existence of the only one interface where as in SIS and SNS contacts we should have two ones).

It is necessary to add that thanks to a intensive reflection of the quasiparticles from the disorder regions their concentration in this area has to fall down resulting in weakening the screening of the Coulomb repulsion. It can be one of the reasons of the intensive temperature independent pair breaking leading to suppression of the critical current of the junctions.

In the wave-guide model [7] the description of this effects can be done in the framework of the Gor'kov equations by introducing two parameters W and λ_0 which are responsible for transparency and the intensity of pair breaking processes at the boundary respectively. The calculations lead to the temperature dependence of I_cR_N product coincides with the one in AB-theory

$$eI_cR_N = \frac{\pi}{2}\Delta_0(T)\,\mathrm{th}\left[\frac{\Delta_0(T)}{2T}\right] \frac{|1 - R_\lambda/R_N|}{(1 + R_\lambda/R_N)^2}, \quad R_N = \frac{6\pi^2 m^2 W^2}{e^2 p_F^4}, \quad R_\lambda = \frac{6\pi^2 m^2 \lambda_0^2}{e^2 p_F^4}. \qquad (13)$$

It is interesting that the increasing of the ratio R_λ/R_N results not only in the suppression of the I_cR_N product but even to the crossover from ordinary junction's behavior to "π"-contact.

5. CONCLUSION.

To understand the data obtained in HTS junctions it is necessary to take into account the finite transparency of the boundaries as well as the temperature independent pair breaking. The pair breaking mechanisms are responsible for the relatively large and temperature independent decay length and suppression of the I_cR_N product at the boundaries of the junctions. The physical reasons leading to the finite boundary transparency in HTS weak links are practically the same as in the single grain boundary junctions. The mismatch of the atomic lattices at the boundaries results in appearance of the intensive mechanical tensions and as a consequence in the lack of the periodicity in *C* direction in its vicinity. It is for this reason the transition from three to two-dimensional types of conductivity has to take place near the boundaries leading to the formation on atomic scale low transparency regions. It is obvious that if it is really so then the I_cR_N product of the weak links with normal oxide interlayers do not exceed the one in single grain boundary junctions. Nevertheless it may be interesting to go forward in this direction since it could open the possibilities to find new effects in the structures with the ferromagnetic interlayers.

REFERENCES

1. Chin P K , and Van Duzer T , (1991) Appl.Phys.Lett. 58: 753
2. Kasai M, Ohno T, Kanke Y et al. (1990) Jpn.J.Appl.Phys. 29: L2219
3. Ying OY, Kwok HS (1990) Appl.Phys.Lett. 56: 1478
4. Hwang DM, Ying QY, Kwok HS (1991) Appl.Phys.Lett. 58: 2429
5. Colino J, Sacedon JL, Vicent JL, (1991) Appl.Phys.Lett. 59: 3327
6. Maysubara G, Matsui T, Okabe Y, (1991) Jpn.J.Appl.Phys. 30: L1796
7. Kupriyanov MY, (1992) In: Koch H, Lubbig H (eds) in: In Superconducting device and their application. Shpringer, Berlin, pp 19-27
8. Gurwich M, Kupriyanov MY (1992) Josephson effect in HTS structures Preprint (to be published).
9. Kupriyanov MY, Likharev KK (1990) Soviet Phys. Uspekhi, 33: 340
10. Kupriyanov MY, Likharev KK (1991) IEEE Trans Magn. 27: 2460
11. Kupriyanov MY, Lukichev VF, (1988) Sov.Phys.JETP 67: 1163
12. Kupriyanov MYu (1990) In Joshi SK, Rao CNR, Subramanyam SV (eds) in:Int. Conf. on Superconductivity - ICSC. World Scientific, Singapore, pp 352-362.
13. Kupriyanov MY, Golubov AA (1989)Zh.Eksp.Teor.Fiz. [Sov. Phys.-JETP] 96: 1420
14. Forrester MG, Talvacchio J, Giavaber JR et al. (1991) IEEE Tran. Mag. 27: 3098
15. Dilorio MS, Yoshizumi S, Yang K-Y et al. (1992) In: Koch H, Lubbig H (eds) in: In Superconducting device and their application. Shpringer, Berlin, pp 120-126
16. Dilorio MS, Yoshizumi S, Yang K-Y et al., (1991) Appl.Phys.Lett. 58: 2552
17. Ono RH, Beall JA, Cromar MW, et al. (1991) Appl.Phys.Lett. 59: 1126
18. Gijs MAM, Giesbers J.B, van Delft FCMJM et al. (1991) Appl.Phys.Lett. 59: 1233
19. Gao J, Aarnink WAM, Gerritsma GJ et al., (1991) Tran. IEEE Magn. 27: 3062 Appl.Phys.Lett. 59: 2754
20. Kabasava U, Tarutani Y, Fukazava T et al. (1991) Jpn.J.Appl.Phys. 33: 1670
21. Tarutani Y, Fukazava T, Kabasava U et al., (1991)ApplPhys.Lett. 58: 2707
22. Gao J Aarnink WAW, Gerritsma GJ, Rogalla H, (1990) Physica C 171:126
23. Polturak E, Koren G, Cohen D et al. (1991) Phys Rev.Lett. 67: 3038
24. Hunt BD, Foote MC, Bajuk LJ, (1991) Appl.Phys.Lett. 59 982
25. Rogers CT, Inam A, Hegde MS et al. (1989) Appl.Phys.Lett. 55: 2032
26. Barner JB, Rogers CT, Inam A et al. (1991) Appl.Phys.Lett. 59: 742
27. Kasai M, Ohno T, Kanke Y, et al. (1990) Jpn.J.Appl.Phys. 29: L2219
28. Buzdin AI, Kupriyanov MYu (1991) Pis'ma Zh. Eksp.Teor.Fiz. 53: 308